RING CURRENT TIME EVOLUTION DURING A GEOMAGNETIC STORM

Stefano Orsini, Anna Milillo, Alessandro Mura
(Istituto di Fisica dello Spazio Interplanetario, CNR, Roma, Italy)

Yannis A. Daglis
(Institute of Space Research National Observatory of AthensMetaxa and Vas. Pavlou Str.15236 P. Penteli, Greece)

ABSTRACT **- THE ION SPECTRA TIME EVOLUTION AND THE ROLE OF CHARGE-EXCHANGE DECAY DURING THE RECOVERY PHASE OF A GEOMAGNETIC STORM OCCURRED ON JUNE 4-7 1991 ARE DISCUSSED.**

PROTON AND OXYGEN ION SPECTRA FROM CRRES MICS EXPERIMENT, AS OBTAINED WITH 10-HOUR STEPS AT R = 4 RE AND MLT = 1600 ARE ANALYZED. DURING A 10 HOURS INTERVAL WHEN A CLEAR SIGNATURE OF THE OCCURRENCE OF THE RECOVERY PHASE IS IDENTIFIED, THE AVAILABLE FLUX SPECTRA AT DIFFERENT PITCH ANGLES ARE SHOWN. ON EACH SPECTRUM THE CHARGE EXCHANGE DECAY RATE IS APPLIED, IN ORDER TO ESTIMATE THE RELEVANCE OF THIS PROCESS WITH RESPECT TO OTHER POSSIBLE LOSS MECHANISMS. THE RESULTING SPECTRA ARE COMPARED TO THE SIGNAL OBSERVED BY THE INSTRUMENT AFTER THE CHOSEN TIME INTERVAL.

ONCE APPLYING PROPER CHARGE EXCHANGE LOSS RATES TO THE SPECTRA, THE POTENTIALITY OF A RING CURRENT EMPIRICAL MODEL IS TESTED BY ATTEMPTING TO RECONSTRUCT THE TREND OF THE DATA DURING THE STORM DEVELOPMENT. THE STORM MAJOR EFFECTS, LIKE L-SHELL COMPRESSION AND CROSS-TAIL POTENTIAL DROP INCREASE ARE WELL RECONSTRUCTED. USING THE MODEL, THE POSSIBLE GLOBAL SCALE TIME EVOLUTION OF THE RING CURRENT PROTON DISTRIBUTIONS DURING THE SELECTED STORM IS SHOWN AND THE RELATED PHYSICAL IMPLICATIONS ARE BRIEFLY DISCUSSED.

Introduction

During the recovery phase of the magnetospheric substorms, the Earth's ring current, enriched by new plasma injected during the main phase, is subjected to several loss processes. These processes are globally acting on the inner magnetospheric plasma, thus causing a generalized decay of the ion distributions. Actually, it is well known that charge exchange between the energetic ring-current ions and the cold exospheric hydrogen is the dominant loss mechanism in the inner magnetosphere (e.g. Daglis et al., *1999*). All magnetospheric ion populations undergo such a loss process, nevertheless the consequent decay rate is strongly dependent on both ion species and energy. For instance, H^+ ion fluxes are mostly affected by this process at low energy (below 10 keV) On the other hand, O^+-H charge exchange cross sections are instead hardly dependent on ion energy, so that the singly charge oxygen loss rate is relatively high even above 100 keV (see *Orsini et al., 1994*).

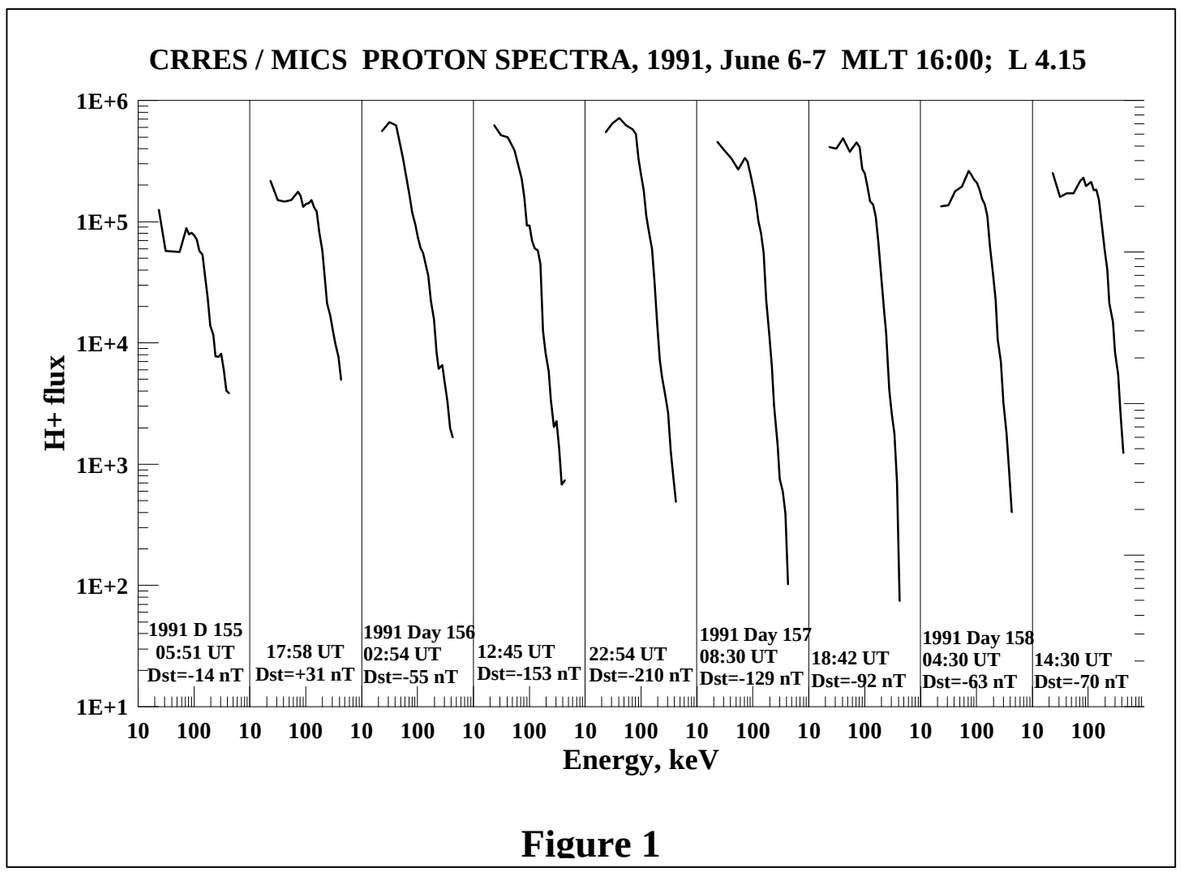

Figure 1

Moreover, the charge exchange decay rate is also dependent on exospheric hydrogen density. It follows that those ions that reach

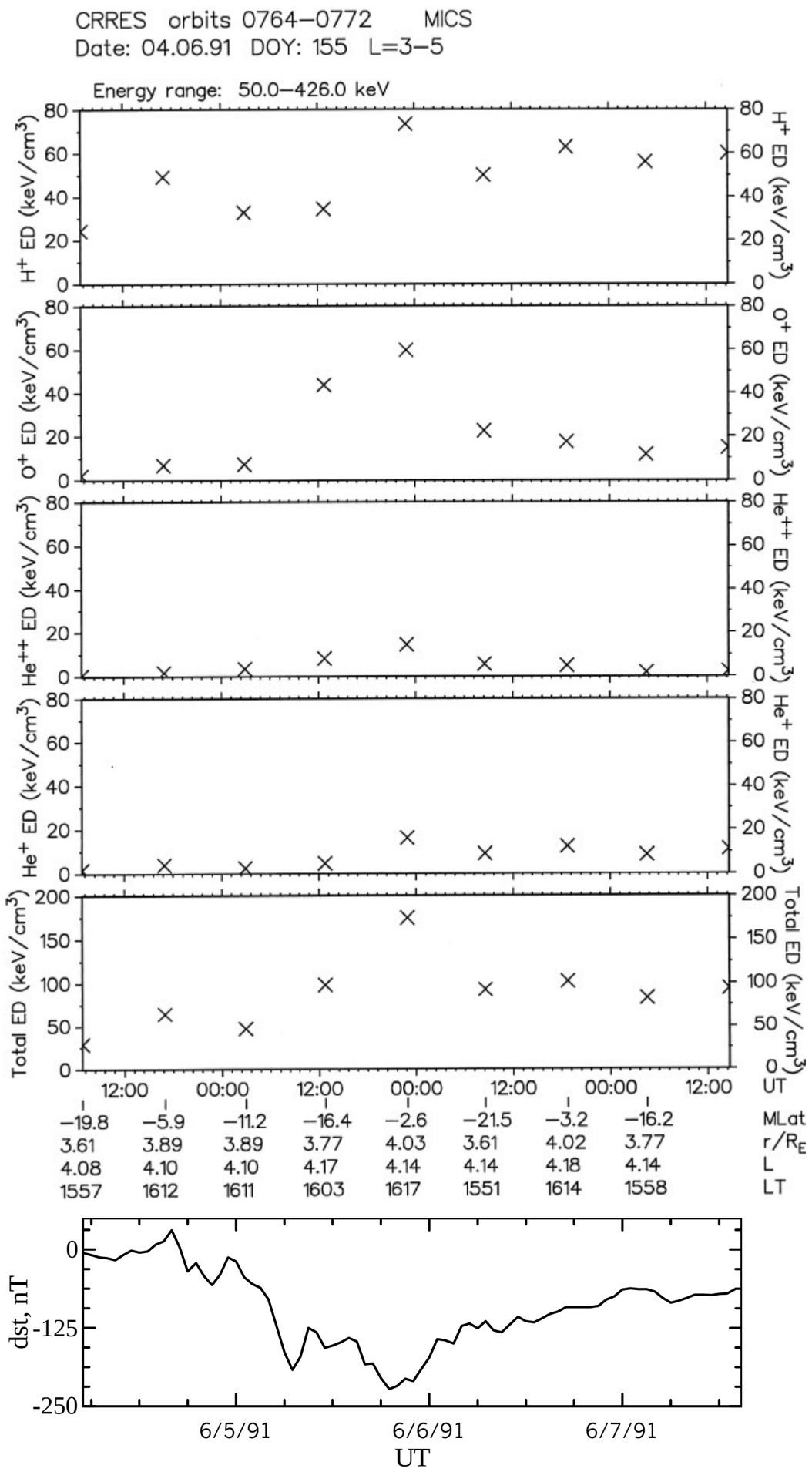

Figure 2

their mirror points at lower altitudes (i.e. with small pitch angles on the magnetic equator) are consequently more affected by this mechanism (see *Smith and Bewtra*, 1978).

Data Analysis

In order to check the relevance of charge exchange loss processes in the decay of H^+ and O^+ energy spectra during the recovery phase of the storm occurred on June 5, 1991, instantaneous ion fluxes from CRRES MICS have been collected with time resolution of ~10 hours (**Figure 1**).

At the times of data detection, the CRRES satellite was roughly located in the Earth's dusk side (~ 16:00 MLT), at an altitude of about 4 R_E.

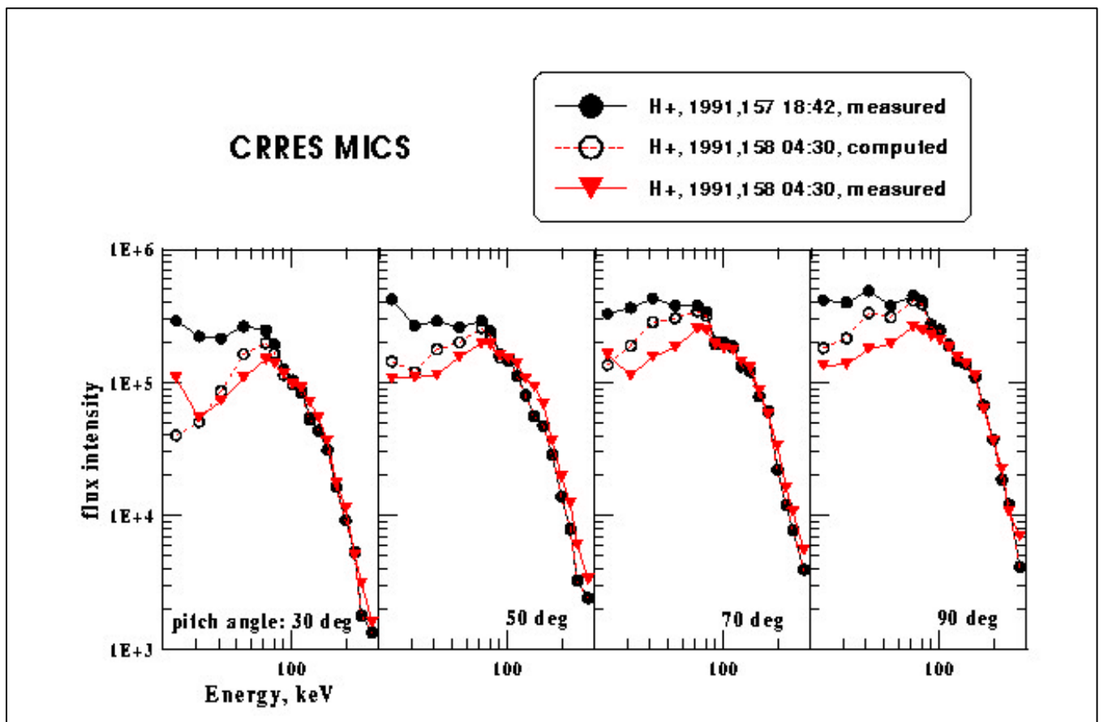

Figure 3

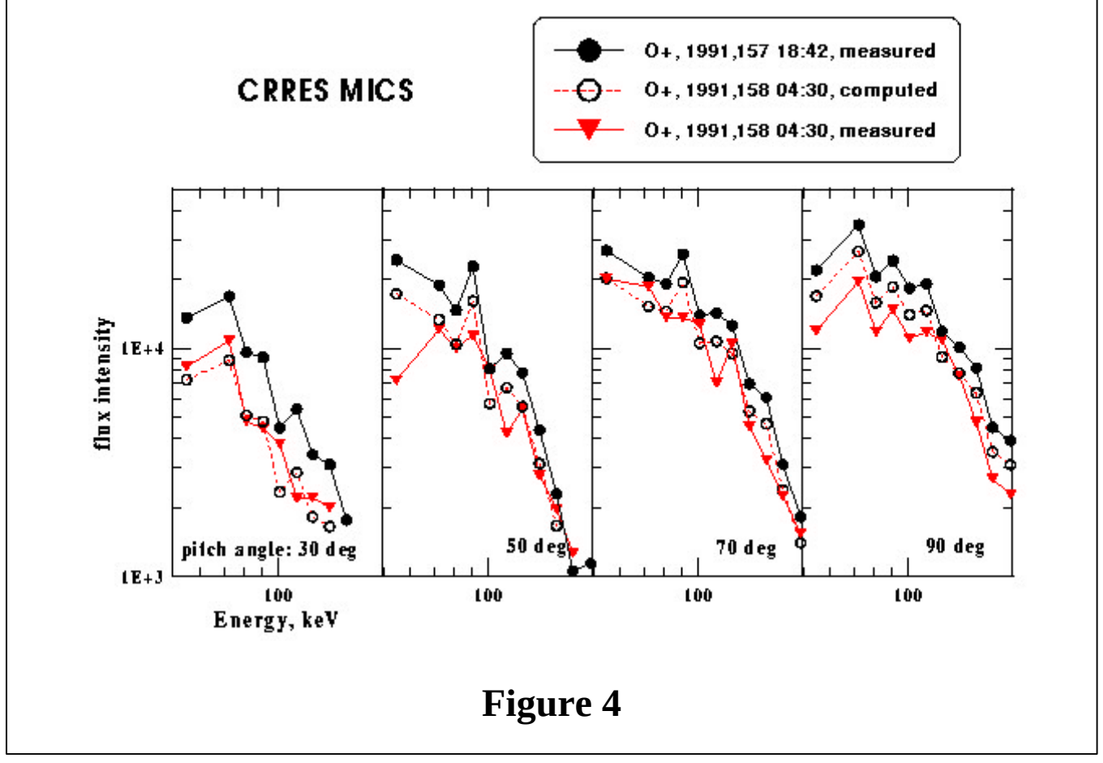

Figure 4

The energy density (ED) profiles versus time are shown in **Figure 2** for an extended time period (from doy 155, 08 UT to doy 158, 14 UT) centered on the storm onset (occurred in the middle of doy 156). By looking at this figure, we notice that an evident smooth decrease of ED, simultaneously for all the considered ion species, is clearly noticeable only between day 157, 18:40 UT and day 158, 04:30 UT (just following the substorm main phase). Conversely, at the same time the Dst index (see bottom of **Figure 2**) smoothly increases (from –92 nT to –63 nT), following the substorm-related abrupt decrease to less than -200 nT. These two features are indicative of the occurrence of a relatively undisturbed recovery phase. In this particular condition, the global decay caused by loss processes should be clearly reflected in the ion flux spectra, although in the case we are considering the collected data set is localized within a limited portion of space. For this reason, we have focused our analysis on the mentioned time interval.

The two consecutive H^+ and O^+ energy spectra, as taken by CRRES MICS in the selected time period, are shown respectively in **Figure 3** (H^+ ions) and **Figure 4** (O^+ ions). In the two figures, black circles connected by thick lines refer to the first spectrum, while triangles and thick lines trace the further one. As indicated in the figures, the four panels refer respectively to four different pitch angles (from 30^0 to 90^0). By looking at the H^+ fluxes, at energies lower than 100 keV and at high pitch angles, the further profiles show flux values that are lower than those previously detected, thus confirming the feeling that the action of the loss processes is dominant in this time interval. Concerning O^+ a clear signal decrease is noticed at all energies.

Charge exchange loss simulation

For simulating the flux spectra evolution caused by the charge exchange effect, we have computed the specific ion loss rate *lr* according to the following expression:

$$\mathbf{lr(E_i,\varphi_j)= \sigma_i\, n_j\, v_i} \qquad (1)$$

where σ_i is the charge-exchange cross section of the chosen ion at energy E_i, n_j is the exospheric hydrogen density at the mirror point altitude (dependent on the equatorial pitch angle φ_j), and v_i is the ion differential velocity (kinetic + thermal) corresponding to energy E_i.

By using expression (1), the reduced ion flux at each energy and pitch angle can be estimated as a function of time t:

$$\mathbf{F_{red}(E_i,\varphi_j,t) = F_0(E_i,\varphi_j,t_0) * (1 - lr(E_i,\varphi_j))^t} \qquad (2)$$

where F_{red} is the charge exchange reduced flux, F_0 is the measured flux at instant t_0, and t is the number of seconds recurred from t_0.

Starting from the spectra observed on doy 157, 18:42 UT, we have simulated the expected spectra at the time of the further detection on doy 158, 04:30 UT. For this simulation, the cross sections and exospheric density values used by Orsini et al. (1994) for simulating the ENA fluxes (resulting from the charge exchange decay process) have been applied. The resulting spectra are shown in **Figure 3** and **Figure 4**, respectively for protons and singly charged oxygen ions (light circles connected by dashed lines).

It is evident that the simulated fluxes are very similar to the observed ones. Concerning the protons, same as for the observed data, the computed fluxes significantly decrease only below 100 keV, whereas the higher energy fluxes are mostly unaffected. Even the simulated O^+ fluxes are not dissimilar from the observed ones: in this case the decay occurs at all energies. Another noticeable feature is the evident trend of the decay rate versus equatorial pitch angle: as expected, the loss rate is more efficient for those particles mirroring at lower altitude (i.e. with smaller pitch angles). This is especially evident when inspecting the 30^0 pitch angle H^+ and O^+ spectra (first panels to the left of **Figure 3** and **Figure 4**). In this case, the simulated data fit almost perfectly the observations. From a more general point of view, it should be noted that the observed fluxes are somehow lower that the expected ones (especially for higher pitch angle distributions); such minor discrepancies could be due to the combined effect of other loss mechanisms. Anyway, these do not seem to be able to produce any major decay effect.

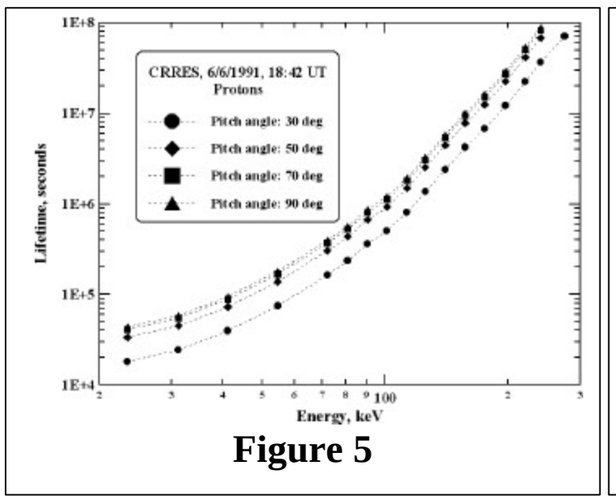

Figure 5

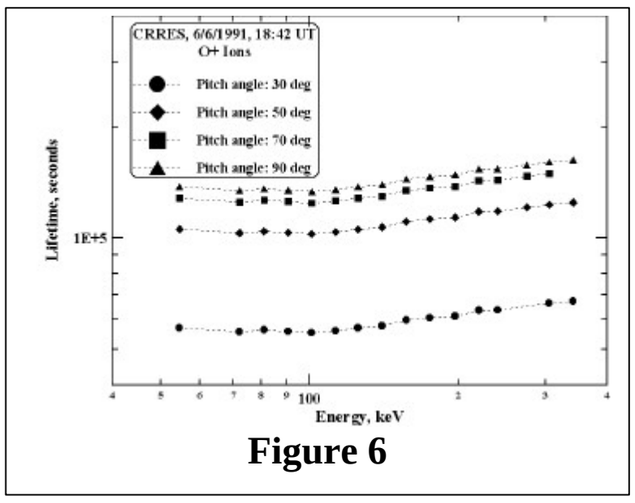

Figure 6

If we assume:

$$\mathbf{F_{red}(E_i,\varphi_j,t) = F_0(E_i,\varphi_j,t_0) * 1/e}$$

then, from (2) we can estimate the charge exchange decay time of the observed spectra. In **Figure 5** and **Figure 6**, such lifetimes are shown as a function of energy for the first of the two spectra analyzed in Figure 3 and 4. By looking at this figure, we can deduce that:

i) at each energy, the lifetime is dependent on pitch angle, so that the closer it is to 90^0, the shorter is the decay lifetime;

ii) at low energy, both H^+ and O^+ lifetimes are less than one day;

iii) at higher energy, O^+ and H^+ lifetimes differ considerably, so that the first one stays constantly around 10^5 s (0.5-2 days), while the second one increases up to 10^8 s (several years).

Previous considerations allow to conclude that charge exchange cannot affect significantly the H^+ fluxes above 7-8 keV, whereas the same mechanism is eventually able to make low energy H^+ and O^+ totally disappear within a few days, in the absence of any ion supply through new injection processes.

Storm-time Ring Current evolution

The empirical model proposed by Milillo et al (1999, 2000) depicts the solar minimum proton flux distributions in the inner geomagnetic equator by means of a functional form, deduced from a statistical best-fit analysis of experimental data (**see also the parent poster by Milillo et al.**). By using such a function, we attempted to best fit the CRRES data reported in **Figure 1**, with the following goals:

1. verify the model ability to depict the *inner magnetospheric plasma* circulation during the selected storm as well as the related field patterns;
2. verify the model ability to identify the *charge-exchange effect* as in the cases shown in **Figure 3**.

Six function parameters have been selected. And their relative variation has been examined by using six corresponding factors. In the following, the six factors and their physical meaning are listed:

- **A**: L-shell modification.
- **B**: Low energy peak intensity. In the basic function, this parameter mainly provides the intensity of the plasma convected by the electric field. The specific energy range implies that also loss processes due to charge exchange should be reflected in the trend of this parameter.
- **C**: Dawn-dusk anisotropy factor. This quantity is strongly connected to the mean energy variation as a function of MLT (related to the electric field intensity, see Milillo et al., 1996)
- **D:** High energy peak intensity factor. In the basic function, this parameter provides the intensity of the plasma trapped by the magnetic field, mostly drifting around the Earth.
- **E:** Low energy distribution width factor.
- **F**: High energy distribution width factor.

Inner magnetospheric plasma

We have successfully fitted the data, and the results are reported in **Figure 7**. The factor profiles versus time as shown at the bottom of the Figure lead to the following conclusions:

1. The L-shell (**A**) moves out of the Earth at the storm main phase, then abruptly reverses its trend at the beginning of the recovery phase (indication of lines stretching and subsequent depolarization?).
2. The dawn-dusk anisotropy (**C**) is higher than 1 throughout the whole storm-time period, thus suggesting an enhancement of the convection electric field. This value is undetermined before as well as after the storm, where it has been artificially set to 1.
3. The low energy peak intensity factor (**B)** increases during the storm main phase (i.e. stronger convection), whereas conversely the high energy peak intensity factor (**D**) decreases (the trapped population is slowed down by this strong convection effect). During the recovery phase, when the convection field relaxes, both the two trends reverse, indicating that the freshly injected particles become trapped and populate the inner magnetosphere

Charge-exchange effect

In **Figure 8** we show the results concerning the two cases presented in **Figure 3**. Two alternative physical scenarios related to the last spectrum (bottom) are compared to the first spectrum (top). The fit shown to the bottom left comes out from the procedure previously described. The other fit (bottom right) makes use of a reduced proton flux, obtained by applying to the functional form the charge exchange erosion process for ten hours.

When comparing the first set of parameters to the two subsequent sets, we may notice that parameter **B** is the most sensitive to the two methods. In the first comparison it decreases form 3.7 to 1.1, thus indicating an abrupt decrease of the intensity of this population. In the second scenario (where charge exchange action is independently included in the model) this parameter does not show such a strong variation.

Hence, we may conclude that the time profile of parameter **B** is able to describe both the injection processes due to convection and the consequent decrease due to charge exchange, when the convection relaxes. Anyway, we should also consider that part of the distribution guided by parameter **B** (especially at higher energy, where the charge-exchange lifetime is longer, see **Figure 5**) should be trapped into closed drift paths during recovery phase, when the cross-tail potential decreases.

MORE RESULTS WILL BE SHOWN DURING THE ORAL PRESENTATION OF STEFANO ORSINI AND ANNA MILILLO.

References

Daglis, I. A., R. M. Thorne, W. Baumjoahn and S. Orsini, The terrestrial ring current: origin, formation and decay, *Rev. of Geophys.*, 37, 407-438, 1999.

Fok, M. -C., J. U. Kozyra, A. F. Nagy, and T. E. Cravens, Lifetime of ring current particles due to Coulomb collisions in the plasmasphere, *J. Geophys. Res.*, 96, 7861, 1991.

Milillo, A., S. Orsini, I.A. Daglis, G. Bellucci, Low-altitude energetic neutral atoms imaging of the inner magnetosphere: a geometrical method to identify the ENA contributions from different magnetospheric regions, *J. Geophys. Res.*, 101, 27123, 1996.

Milillo, A., S. Orsini, I. A. Daglis, and S. Livi, An empirical model of the ion distributions in the equatorial inner magnetosphere, *Phys. & Chem. of the Earth*, 1/3, 209-214, 1999.

Milillo, A., S. Orsini, Y. A. Daglis, Empirical model of proton fluxes in the equatorial inner magnetosphere, *J. Geophys. Res*. ,accepted, 2000.

Orsini, S., I. A. Daglis, M. Candidi, K. C. Hsieh, S. Livi, and B. Wilken, Model calculation of energetic neutral atoms precipitating at low altitudes, *J. Geophys. Res.*, 99, 13489, 1994.

Smith, P. H., and N. K. Bewtra, Charge-exchange lifetimes for ring current ions, *Space Sci Rev.*, 22, 301,1978.

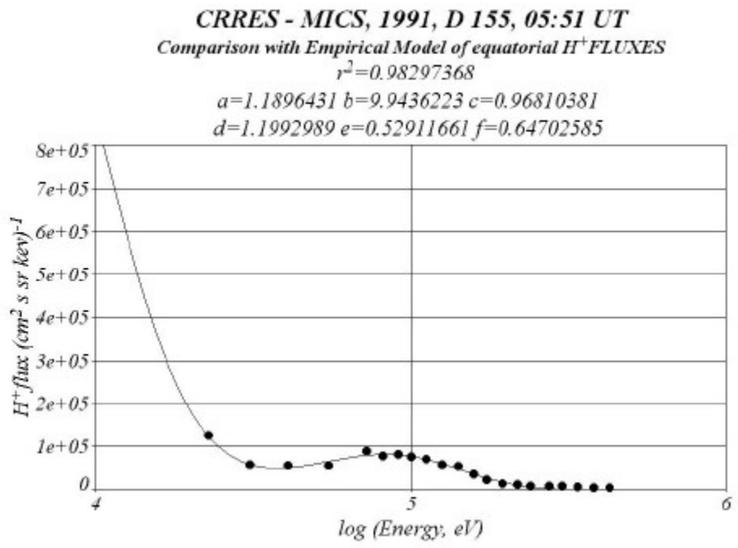

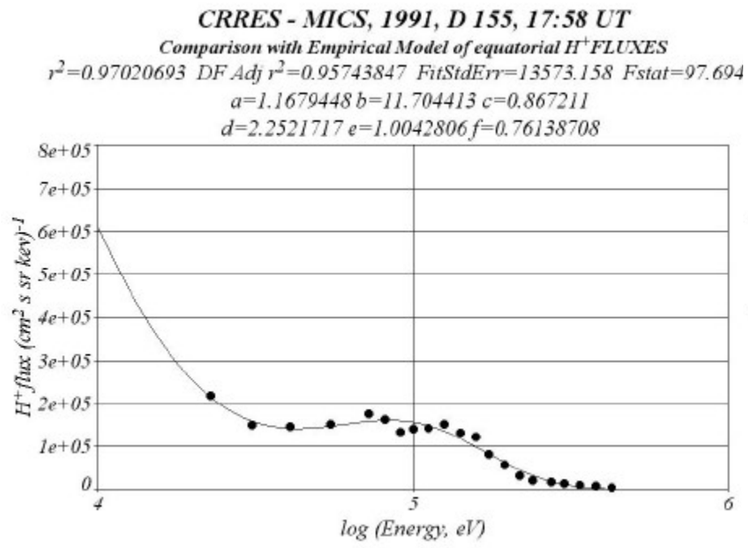

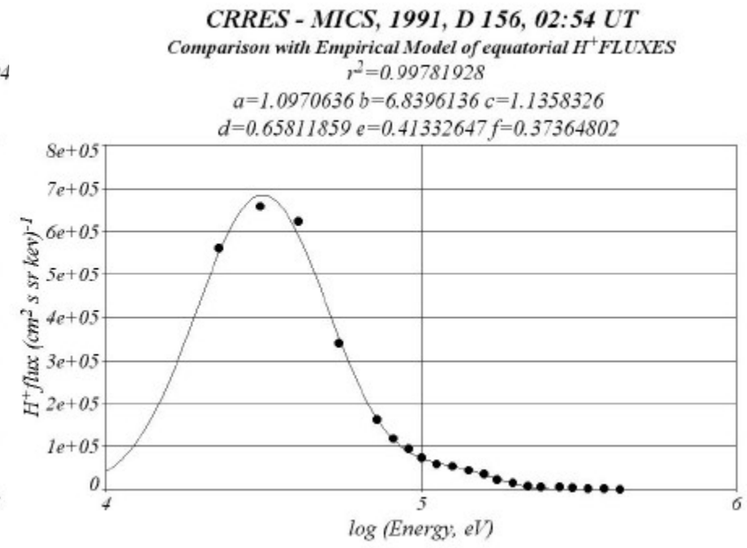

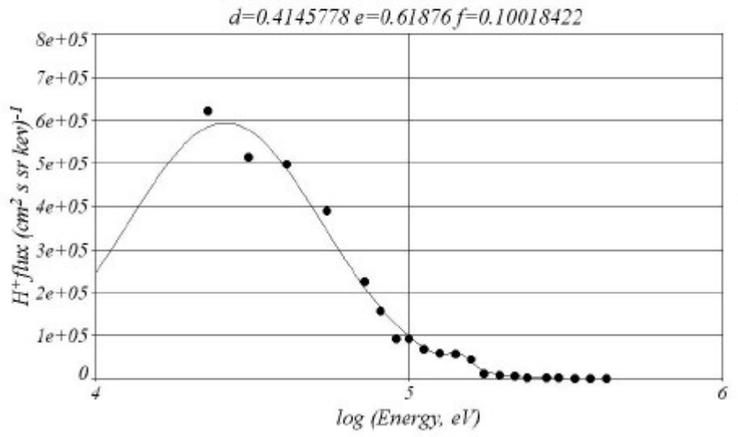

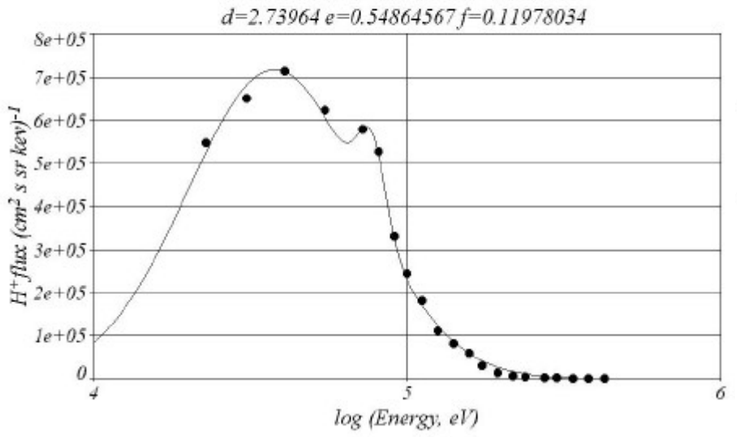

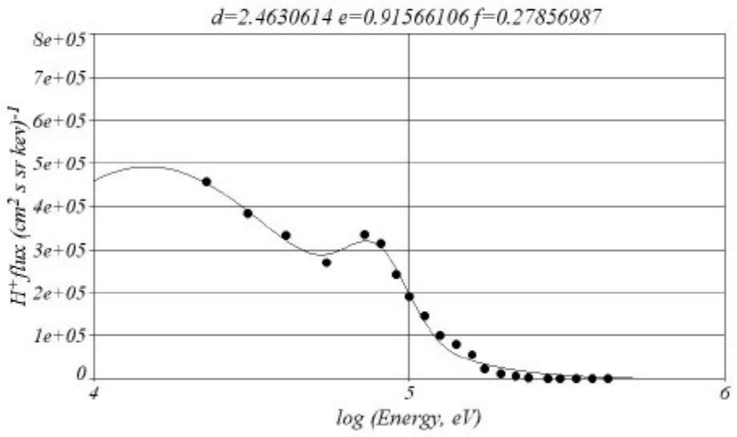

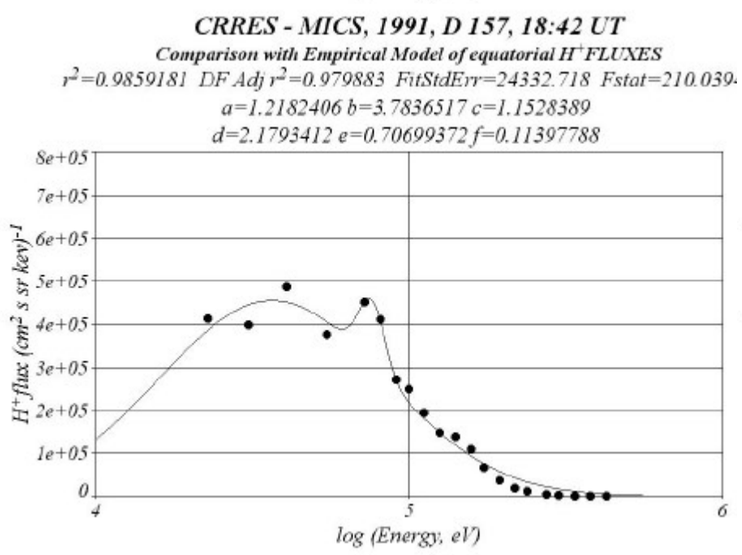

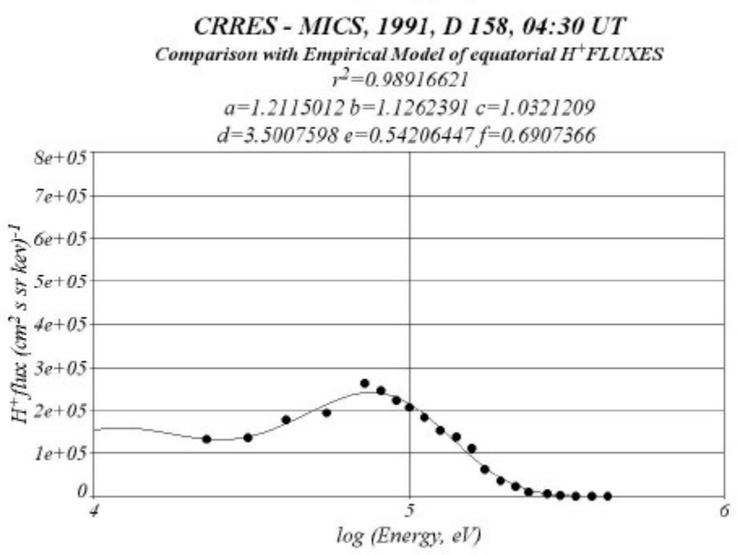

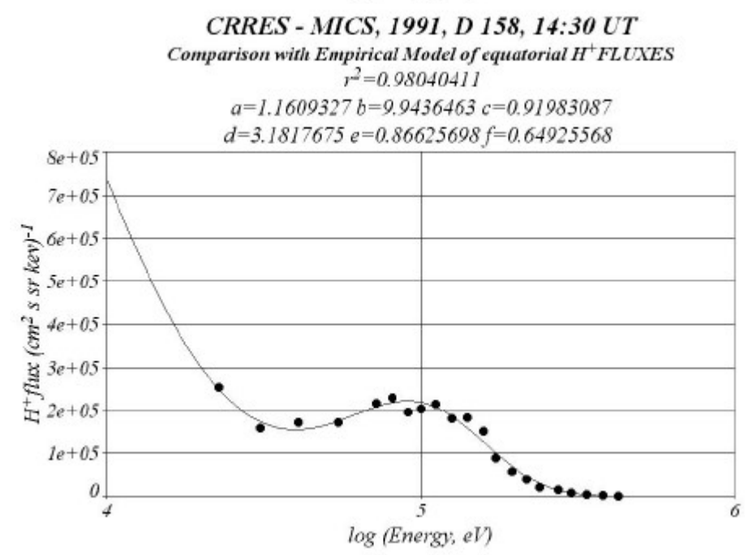

PARAMETER PROFILES

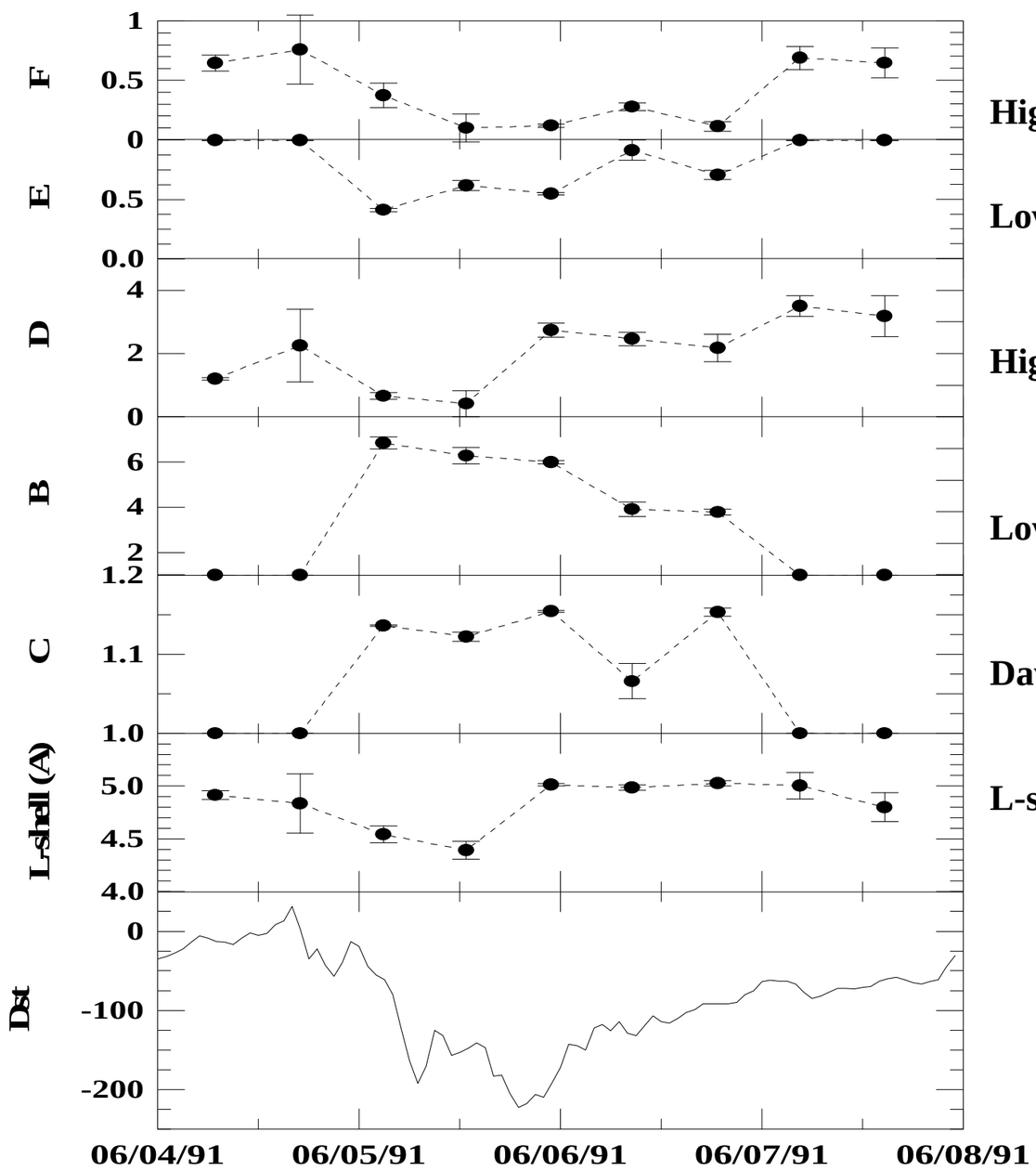

LEGEND

High energy peak width factor

Low energy peak width factor

High energy peak intensity factor

Low energy peak intensity factor

Dawn-dusk asymmetry factor

L-shell variation

Figure 7

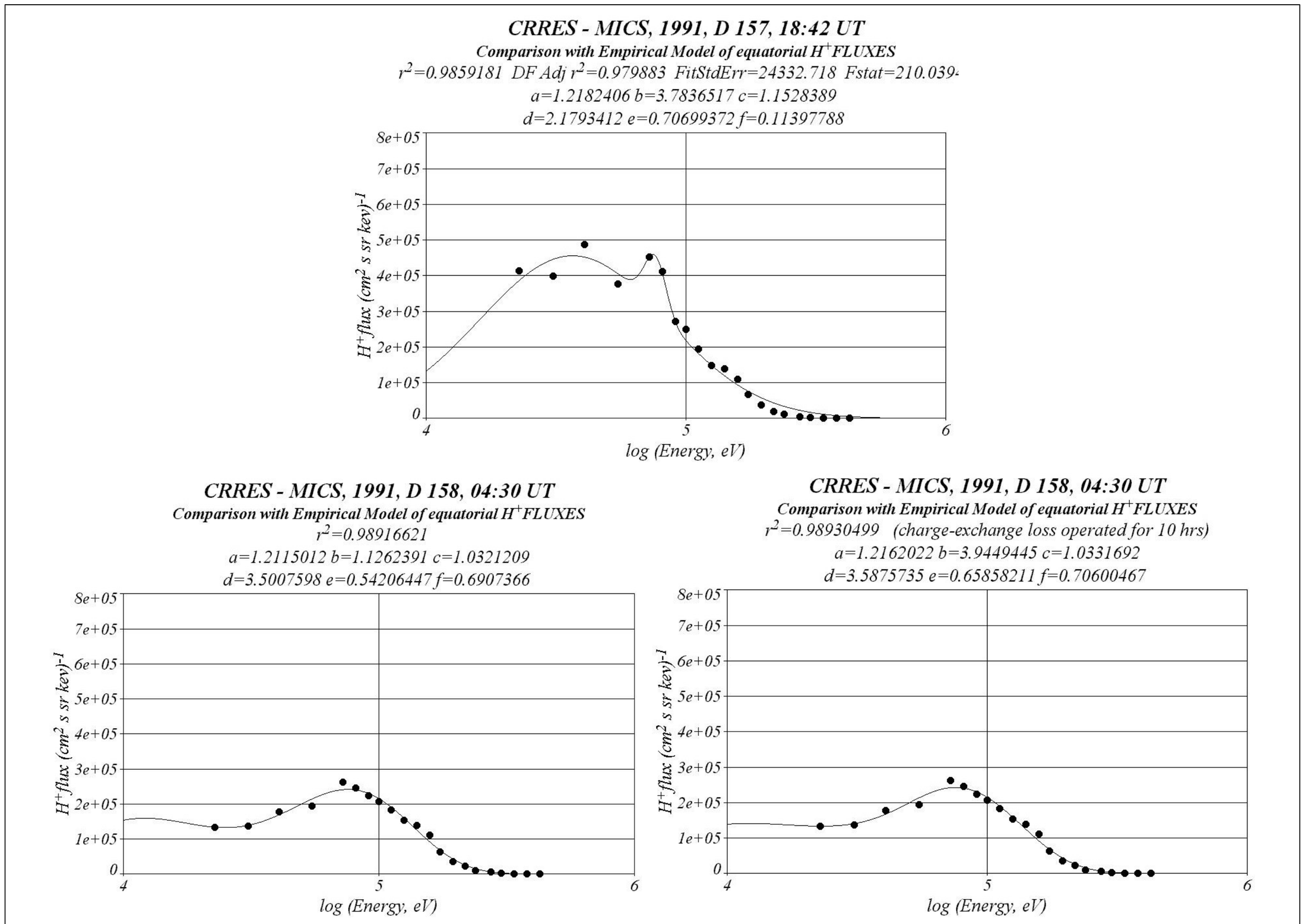

Figure 8

CONCLUSIONS

- WE HAVE EXAMINED THE INSTANTANEOUS H^+ AND O^+ ENERGY SPECTRA FROM CRRES MICS (20 – 500 KEV) DURING THE RECOVERY PHASE OF A MAGNETIC STORM (OCCURRED ON JUNE 5-7, 1991).

- STARTING FROM THE SPECTRA OBSERVED ON DAY 157, 18:42 UT, WE HAVE SIMULATED THE EXPECTED SPECTRA AT THE TIME OF THE FURTHER DETECTION ON DAY 158, 04:30 UT, ASSUMING THAT CHARGE-EXCHANGE WAS THE ONLY ACTING LOSS PROCESS. THE SIMULATED FLUXES ARE VERY SIMILAR TO THE OBSERVED ONES. ACCORDING TO THE EXPECTED LIFETIMES, THE PROTON FLUXES SIGNIFICANTLY DECREASE ONLY BELOW 100 KEV, WHEREAS THE O^+ FLUX DECAY OCCURS AT ALL ENERGIES. THE LOSS RATE IS MORE EFFICIENT FOR THOSE PARTICLES MIRRORING AT LOWER ALTITUDES (I.E. WITH SMALLER PITCH ANGLES).

- THE POTENTIALITY OF A RING CURRENT EMPIRICAL MODEL [MILILLO ET AL., 2000] HAS BEEN TESTED BY ATTEMPTING TO RECONSTRUCT THE TREND OF THE DATA DURING THE STORM DEVELOPMENT. WE HAVE BEEN ABLE TO REPRODUCE THE DATA BY BEST-FITTING SIX PARAMETERS OF THE MODEL. THE PROFILES OF SUCH PARAMETERS DEPICT THE STORM-TIME EVOLUTION OF THE RING CURRENT IN TERMS OF FRESH ION INJECTION, CHARGE-EXCHANGE LOSS, MAGNETIC FIELD VARIATIONS, AND CROSS-TAIL ELECTRIC FIELD ENHANCEMENT.